ISR-MA/BA/JPG/KNH/rh

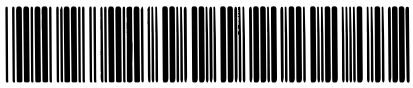

4th June 1971

ISR RUNNING-IN

Run 67 - 9 June 1971 - Rings 1 + 2 - 26 GeV/c - 4 bunches

Run 68 - 9 June 1971 - Rings 1 + 2 - 26 GeV/c - 20 bunches

1. Run 67 - Rings 1 + 2 - BARE MACHINE + 26 SA

The PFW currents which compensate the saturation (file 26 SA of run 53) were added in the two rings.

1.a) Closed orbits

The closed orbits of both machines were first measured without correction, then corrected with the currents of file C026 (see Figs. 8 and 11) on the basis of run 53, and finally re-measured. The characteristics of their distortions expressed in mm are listed in Tables 1 and 2. Their graphs are plotted in Figs. 1 to 4. These corrections were left in the two rings during runs 67 and 68.

Table 1

Ring 1 - Closed Orbits

Orbit	Horizontal		Vertical	
Distortion	peak-to-peak	r.m.s	peak-to-peak	r.m.s.
without correction	7.5	1.7	12.5	2.9
with correction	5.8	1.2	4.6	1.2

Table 2

Ring 2 - Closed Orbits

without correction	21.3	5.9	11.1	3.1
with correction	7.4	1.7	4.5	1.0

1.b) Q measurements in Ring 1

Table 3 gives the results. The corresponding working line is shown in Fig. 5.

Table 3

Ring 1 - Bare machine + 26 SA + C026

<Δr> mm	Q_H	Q_V
inj.	8.802	8.722
-10	.813	.732
C0	.828	.724
+10	.848	.707
+20	.870	.694
+30	.891	.676
+40	.911	.658
+45		.647

2. Run 67 - Ring 1 - FS26 (1.45, 0.85)

To remove a major part of the Q's versus momentum dependence, a sextupole correction ($\Delta Q'_H$ = -4; $\Delta Q'_V$ = +3.15) was added using the PFW ($\Delta G'L_F$ = -81.6 T/m and $\Delta G'L_D$ = -8.4 T/m). Q_H and Q_V became rather constant beyond the central orbit (see Table 4).

<Δr> mm	Q_H	Q_V
-40	8.891	8.643
inj.	.871	.664
-20	.847	.697
-10	.837	.707
C0	.835	.715
+10	.826	.723
+20	.829	.723
+30	.827	.725
+40	.827	.729
+45	.828	.730
+50	.832	.729

Table 4

Ring 1 - Bare machine + 26 SA and $\Delta Q'_H$ = -4 and $\Delta Q'_V$ = +3.15

Then, to obtain the line FS26, the following corrections were added to the previous conditions:

$\Delta Q_H = -0.212$ $\Delta Q_V = -0.116$ $\Delta Q'_H = +1.45$ $\Delta Q'_V = +0.85$

using the PFW and sextupoles:

$\Delta GL_F = -15.846$ T $\Delta GL_D = -11.723$ T

$I_{SF} = 17.01$ % $I_{SD} = 13.14$ %

In addition, the currents in the poleface windings F1, F2 and F3 were adjusted empirically to linearise the working line in the injection region.

The final PFW and sextupole currents are contained in file FS26. The Q values and the scan are given in Figs. 6 and 8.

3. Run 68 - Ring 2 - QC26

The sextupole corrections $\Delta G'L_F = -81.6$ T/m and $\Delta G'L_D = -8.4$ T/m had been estimated from results of measurements in Ring 1 and added to the saturation compensation (26SA). This resulted in the Q values shown in Fig. 9. Additional sextupole corrections of $\Delta G'L_F = 29.5$ T/m and $\Delta G'L_D = 20.4$ T/m were applied together with the octupole corrections $\Delta G''L_F = -1380$ T/m^2 and $\Delta G''L_D = 850$ T/m^2. This resulted in the values shown in Fig. 10. The final adjustment of the PFW currents were calculated using the method of successive approximation. The PFW currents and the Q values are shown in Fig. 11.

4. Run 68 - Ring 2 - SF26 (3.1, 3.5)

The quadrupole corrections $\Delta GL_F = 1.34$ T and $\Delta GL_D = 2.56$ T were added to the point QC26. $Q'_H = 3.1$ and $Q'_V = 3.5$ were added by $I_{SF} = 41$ % and $I_{SD} = 43.4$ %, yielding the working line shown in Fig. 12. $\Delta Q_H = \Delta Q_V = 0.02$ was added and resulted in the working line SF26 (dotted) shown in Fig. 12. A beam loss of 4 % occurred at the resonance $4\,Q_V = 35$ and a total loss of 21 % occurred when crossing the series of 5th order resonances. The power supply settings were filed as SF26 and are shown in Fig. 12.

5. Run 68 - Ring 1 - SF26 (3.1, 3.5)

The same power supply settings were applied in Ring 1 later during run 68 resulting in the working line SF26 shown in Fig. 7.

6. Run 68 - Ring 2 - FS26

An attempt to create FS26 resulted in the working line as shown in Fig. 13. A total beam loss of 18 % occurred when crossing the series of 5th order resonances. There was no time to improve the shape of this line.

B. Autin
J.P. Gourber
K.N. Henrichsen

Distribution:

Prof. K. Johnsen
ISR Group Leaders
Running-in Executive Committee
Engineers-in-Charge
Sc.staff ISR-MA
Mr. M. Höfert HP
Mr. E. Brouzet MPS

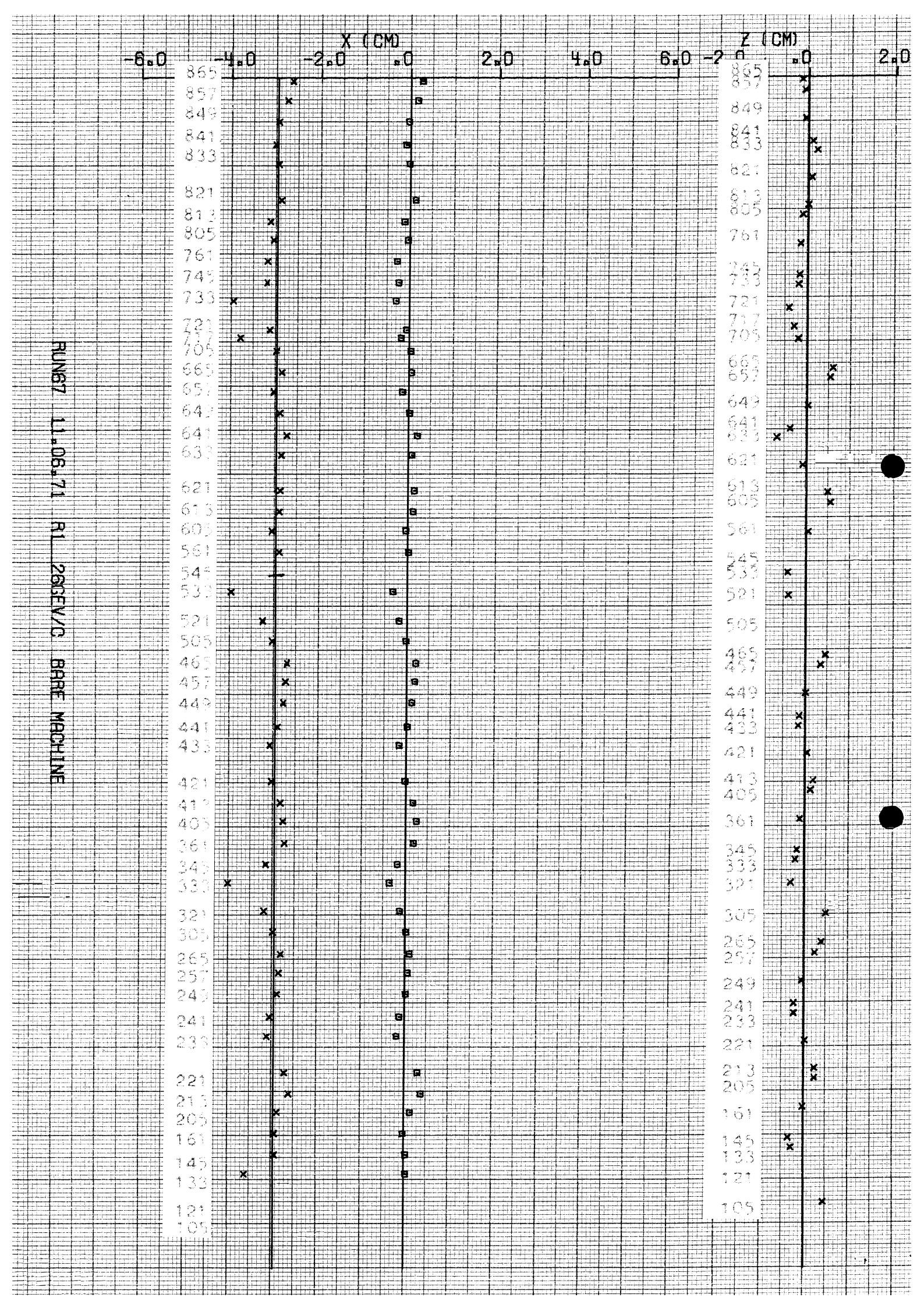
X (CM)
-6.0
-4.0
-2.0
.0
2.0
4.0
6.0
Z (CM)
-2.0
.0
2.0
RUN67 11.06.71 R1 26SEV/C BARE MACHINE

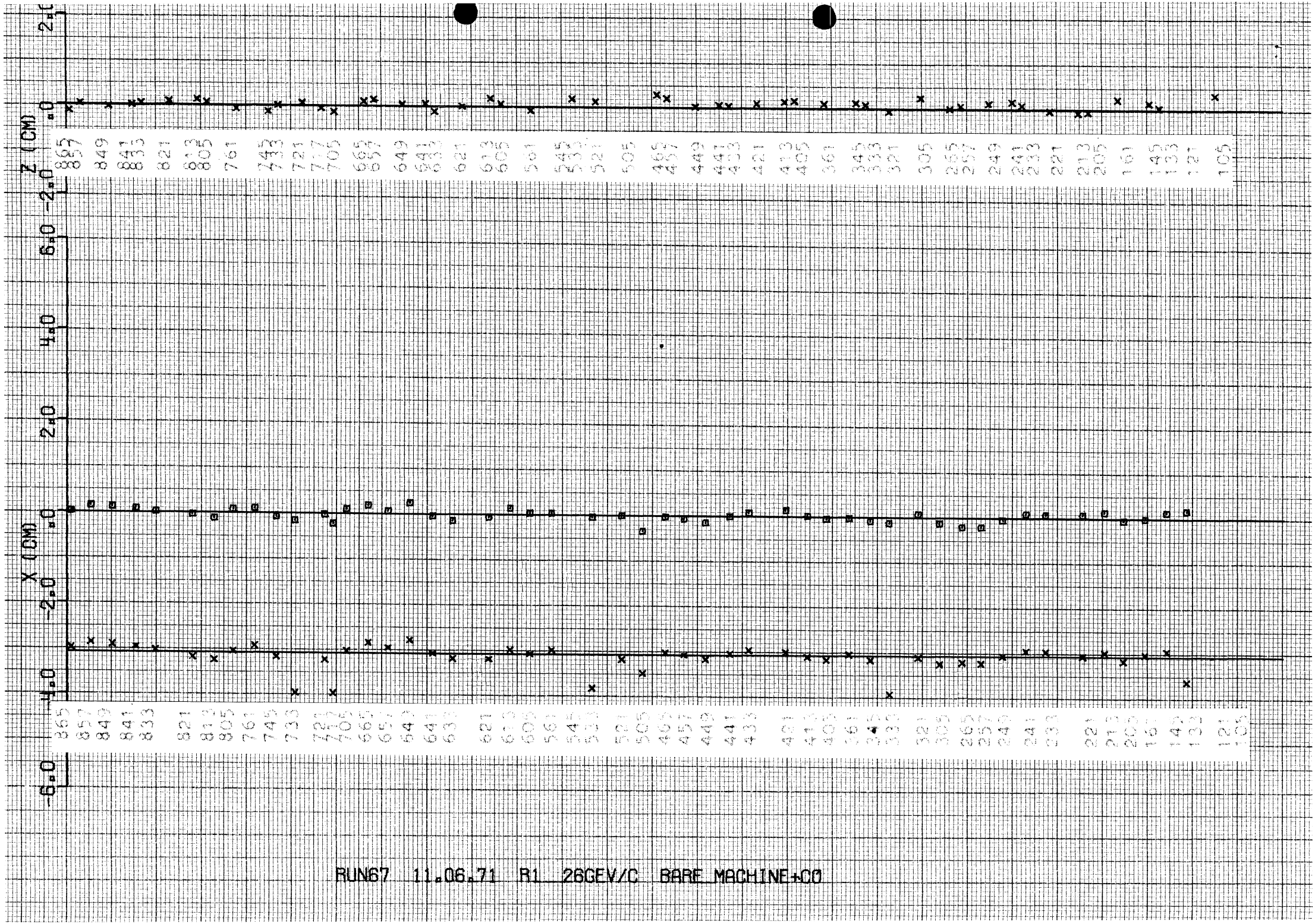
Z (CM)
2.0
0.0
-2.0
X (CM)
6.0
4.0
2.0
0.0
-2.0
-4.0
-6.0
RUN67 11.06.71 R1 26GEV/C BARE MACHINE+CO

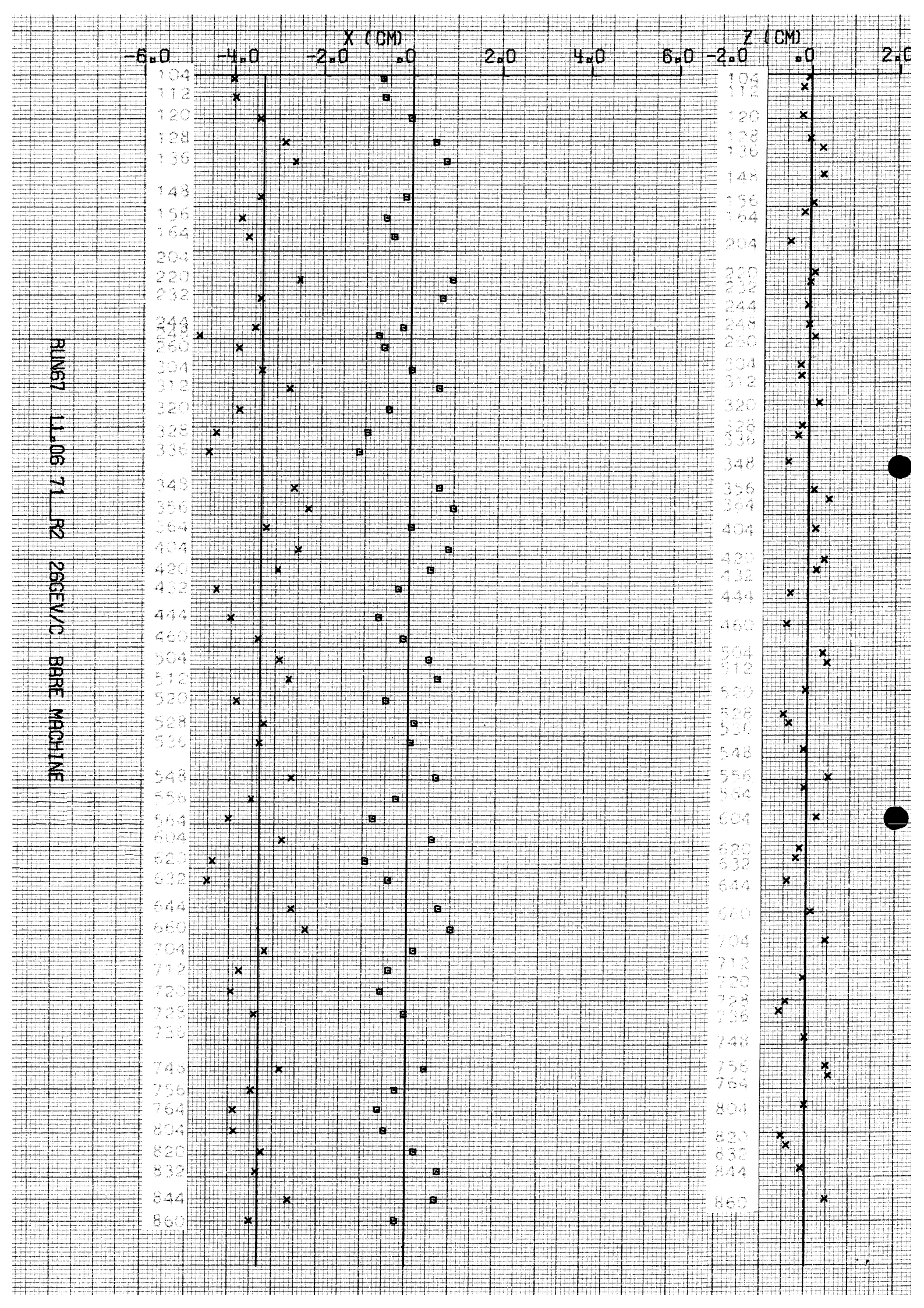
X (CM)
-6.0
-4.0
-2.0
.0
2.0
4.0
6.0
Z (CM)
-2.0
.0
2.0
RUN67 11.06.71 R2 26GEV/C BARE MACHINE


Z (CM)
2.0
0.0
-2.0
X (CM)
6.0
4.0
2.0
0.0
-2.0
-4.0
-6.0
RUN67 11.06.71 R2 26GEV/C BARE MACHINE+CO

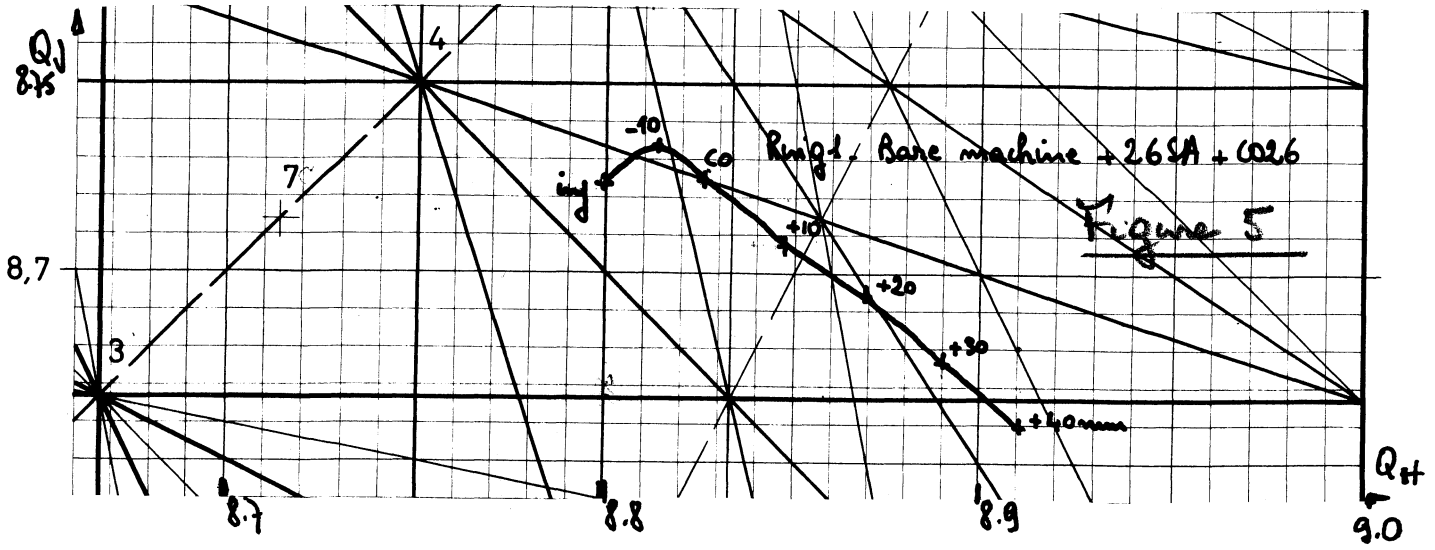

Ruhig 1 - Base machine + 26 SA + CO26

Figure 5

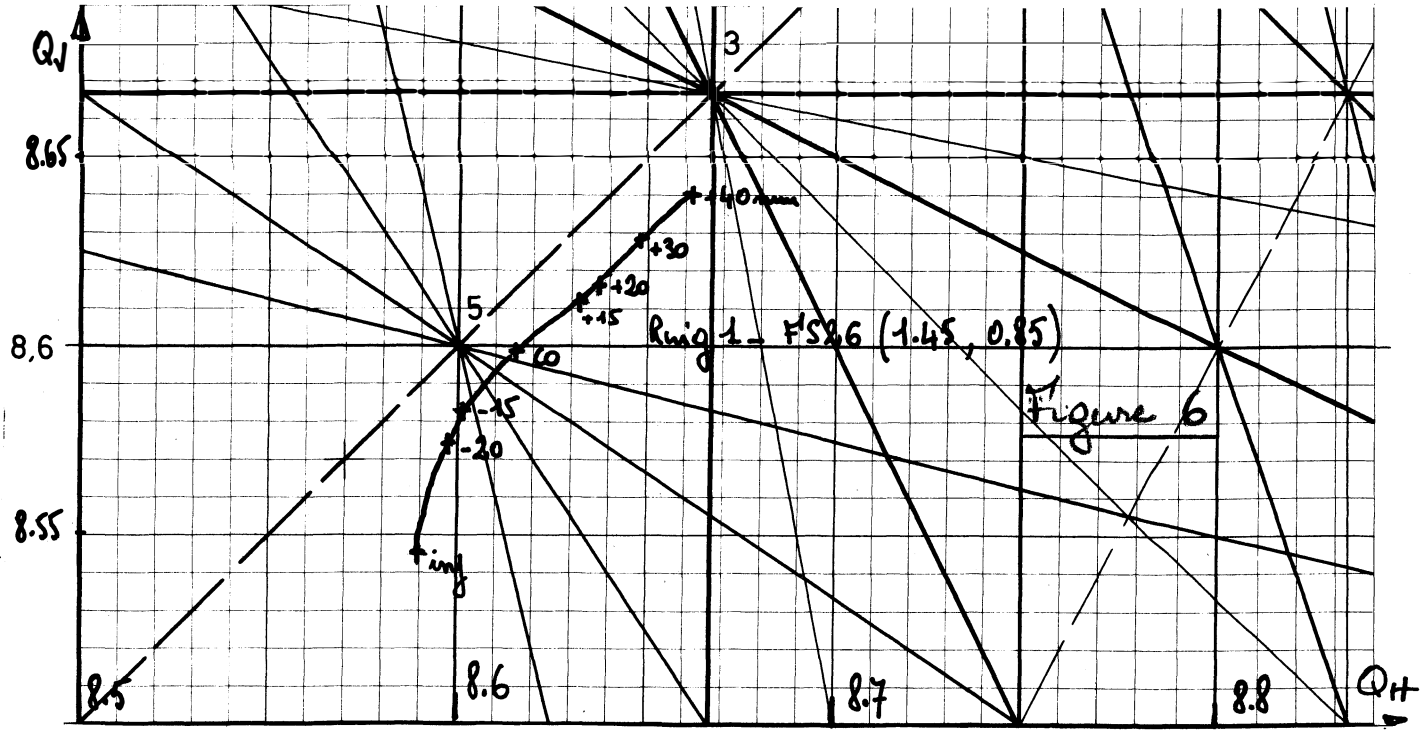

Ruhig 1 - FS26 (1.45, 0.85)

Figure 6

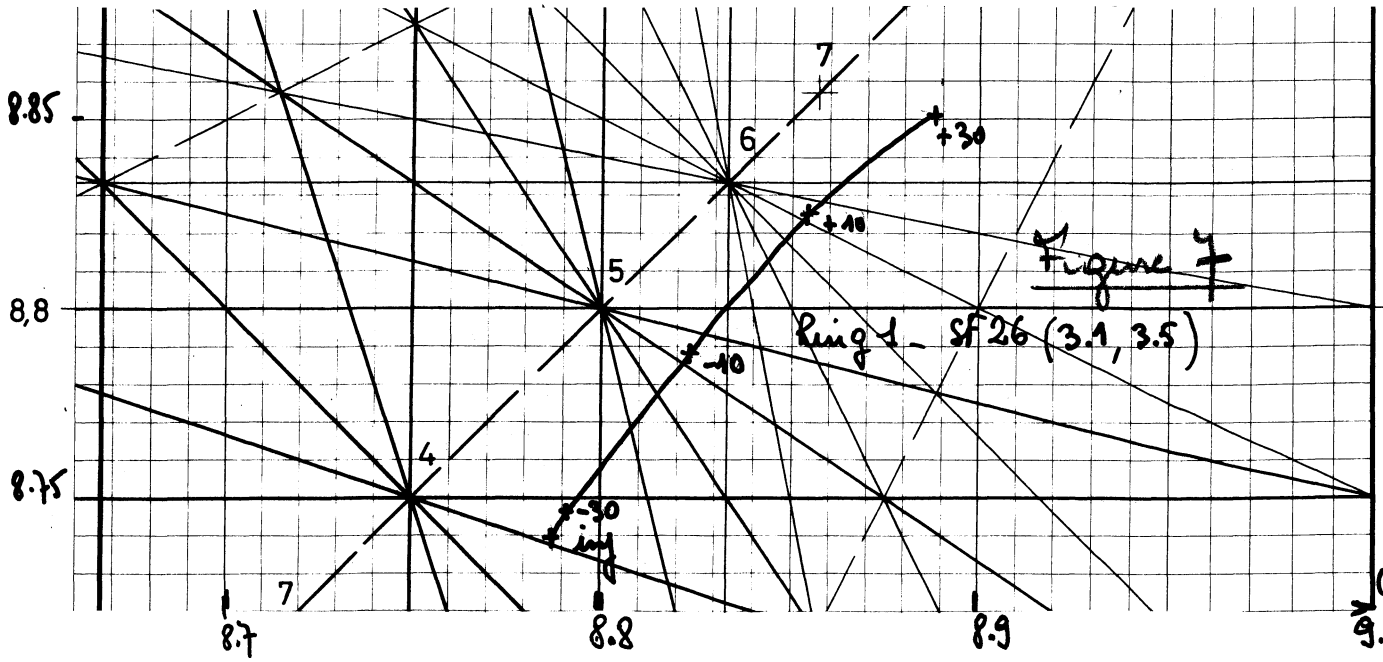

Figure 7

Ruhig 1 - SF26 (3.1, 3.5)

Figure 8 - Run 67. Rung 1. FS26

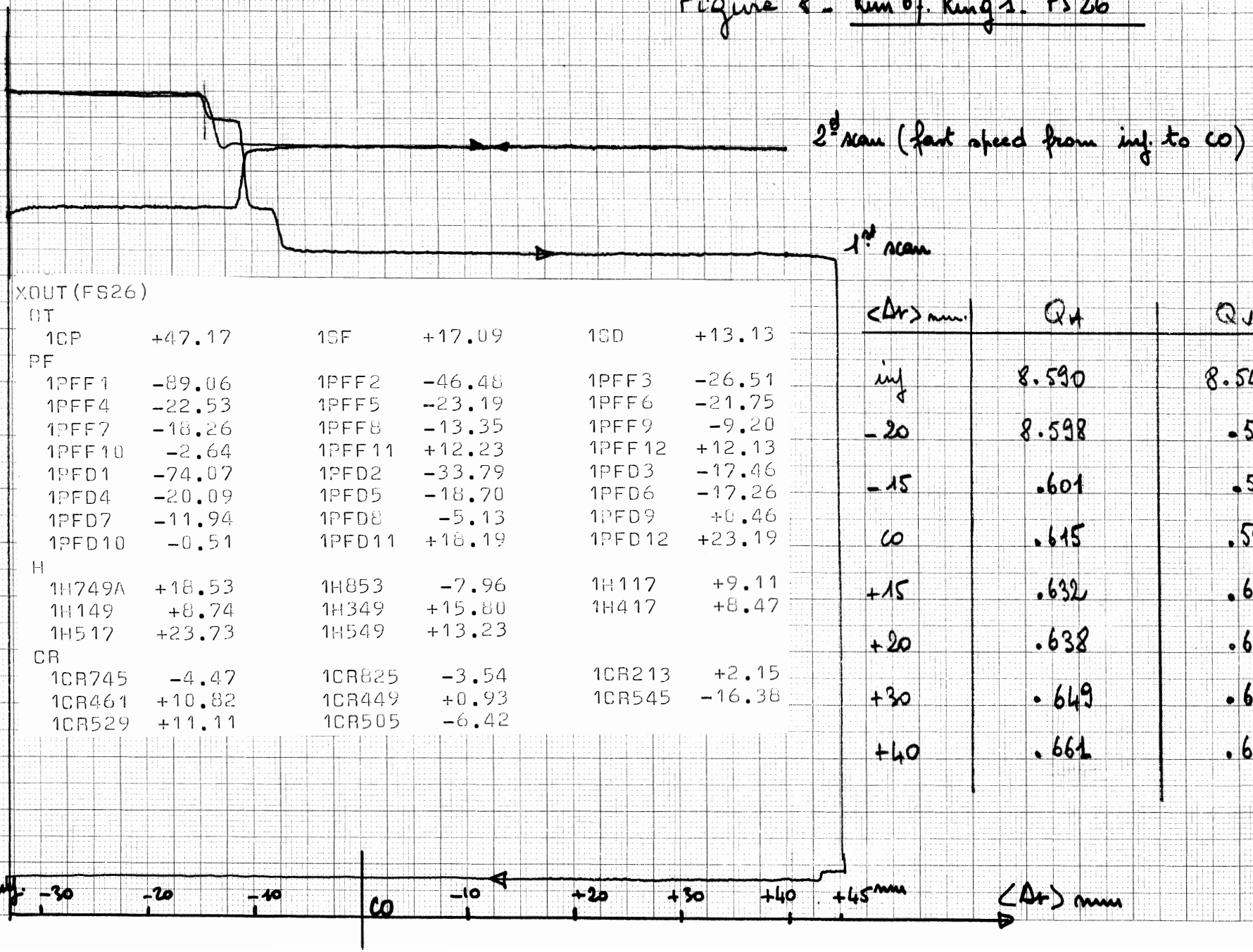

XOUT(FS26)

OT					
1CP	+47.17	1SF	+17.09	1SD	+13.13
PF					
1PFF1	-89.06	1PFF2	-46.48	1PFF3	-26.51
1PFF4	-22.53	1PFF5	-23.19	1PFF6	-21.75
1PFF7	-18.26	1PFF8	-13.35	1PFF9	-9.20
1PFF10	-2.64	1PFF11	+12.23	1PFF12	+12.13
1PFD1	-74.07	1PFD2	-33.79	1PFD3	-17.46
1PFD4	-20.09	1PFD5	-18.70	1PFD6	-17.26
1PFD7	-11.94	1PFD8	-5.13	1PFD9	+0.46
1PFD10	-0.51	1PFD11	+18.19	1PFD12	+23.19
H					
1H749A	+18.53	1H853	-7.96	1H117	+9.11
1H149	+8.74	1H349	+15.80	1H417	+8.47
1H517	+23.73	1H549	+13.23		
CR					
1CR745	-4.47	1CR825	-3.54	1CR213	+2.15
1CR461	+10.82	1CR449	+0.93	1CR545	-16.38
1CR529	+11.11	1CR505	-6.42		

⟨Δr⟩ mm	$Q_\uparrow$	$Q_\downarrow$
inf.	8.590	8.545
-20	8.598	.574
-15	.601	.582
CO	.615	.599
+15	.632	.611
+20	.638	.615
+30	.649	.627
+40	.661	.640

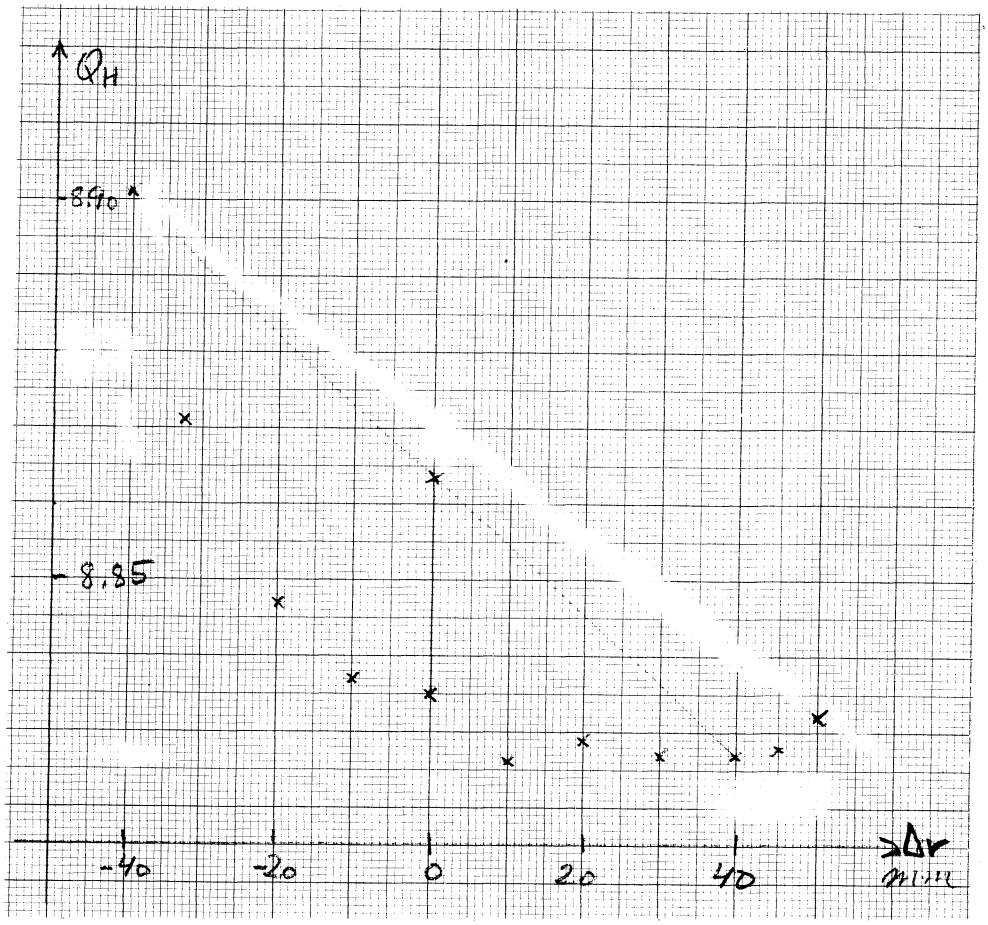

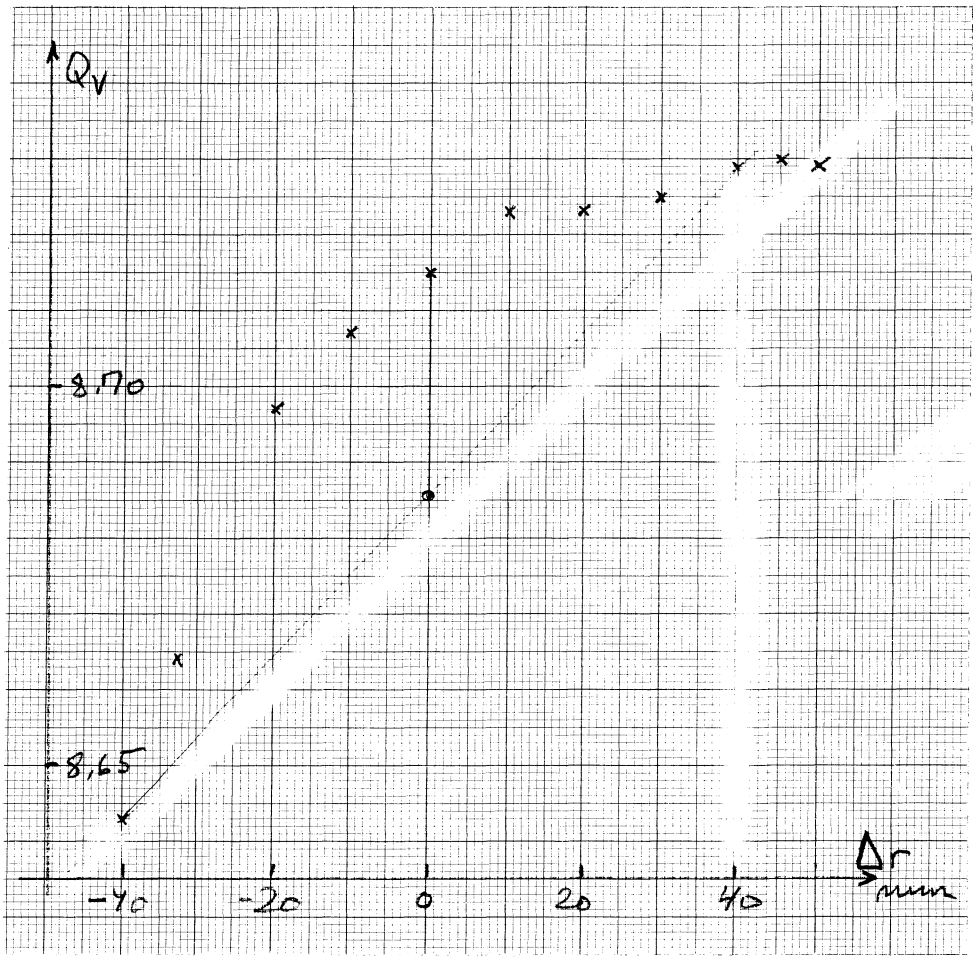

FIG. 9 - Run 68 - Ring 2 -

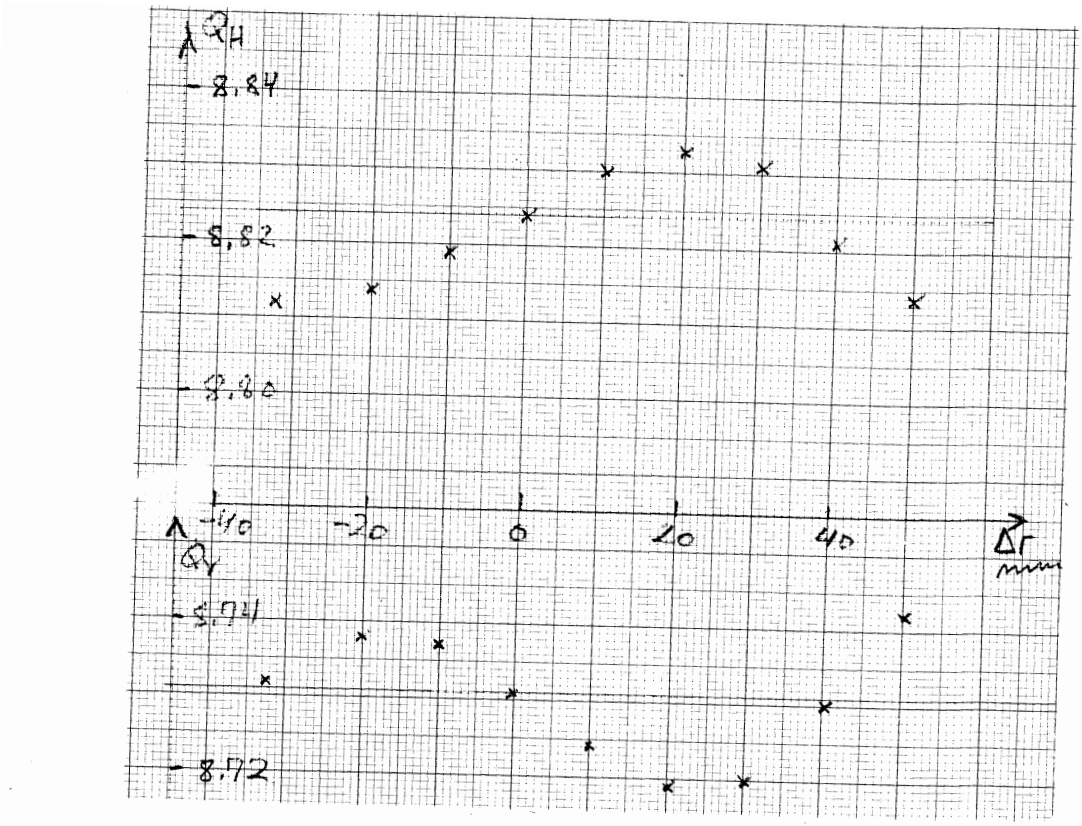

FIG. 10 Run 68 - Ring 2

QC 26

DT								
	2CP	+42.85						
PF								
	2PFF1	-9.18		2PFF2	+1.39		2PFF3	+4.30
	2PFF4	+13.78		2PFF5	+11.30		2PFF6	+9.40
	2PFF7	+8.25		2PFF8	+9.74		2PFF9	+12.99
	2PFF10	+9.81		2PFF11	+22.31		2PFF12	+18.82
	2PFD1	+18.80		2PFD2	+4.20		2PFD3	+1.03
	2PFD4	-0.59		2PFD5	+7.54		2PFD6	+7.35
	2PFD7	+5.91		2PFD8	+15.06		2PFD9	+19.78
	2PFD10	+13.56		2PFD11	+34.52		2PFD12	+34.94
H								
	2H216B	+7.10		2H316	-12.89		2H416	+8.98
	2H716	+4.36		2H848	+10.84			
CR								
	2CR532	+9.12		2CR316	+3.20		2CR320	+3.10
	2CR4	-2.58		2CR5N8	-6.08		2CR532	+2.76
	2CR1N	-3.62		2CR48	+10.45		2CR708	+3.30
	2CR708	-2.88						

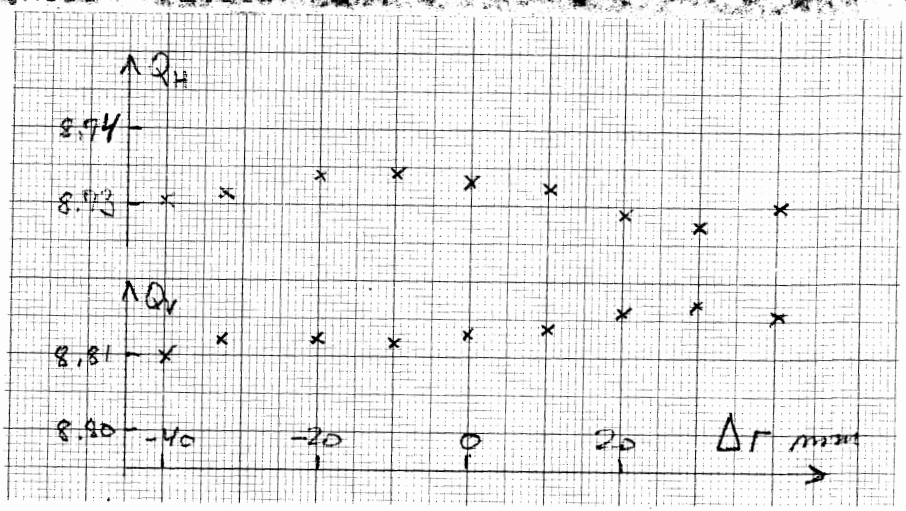

FIG. 11 - Run 68 - Ring 2

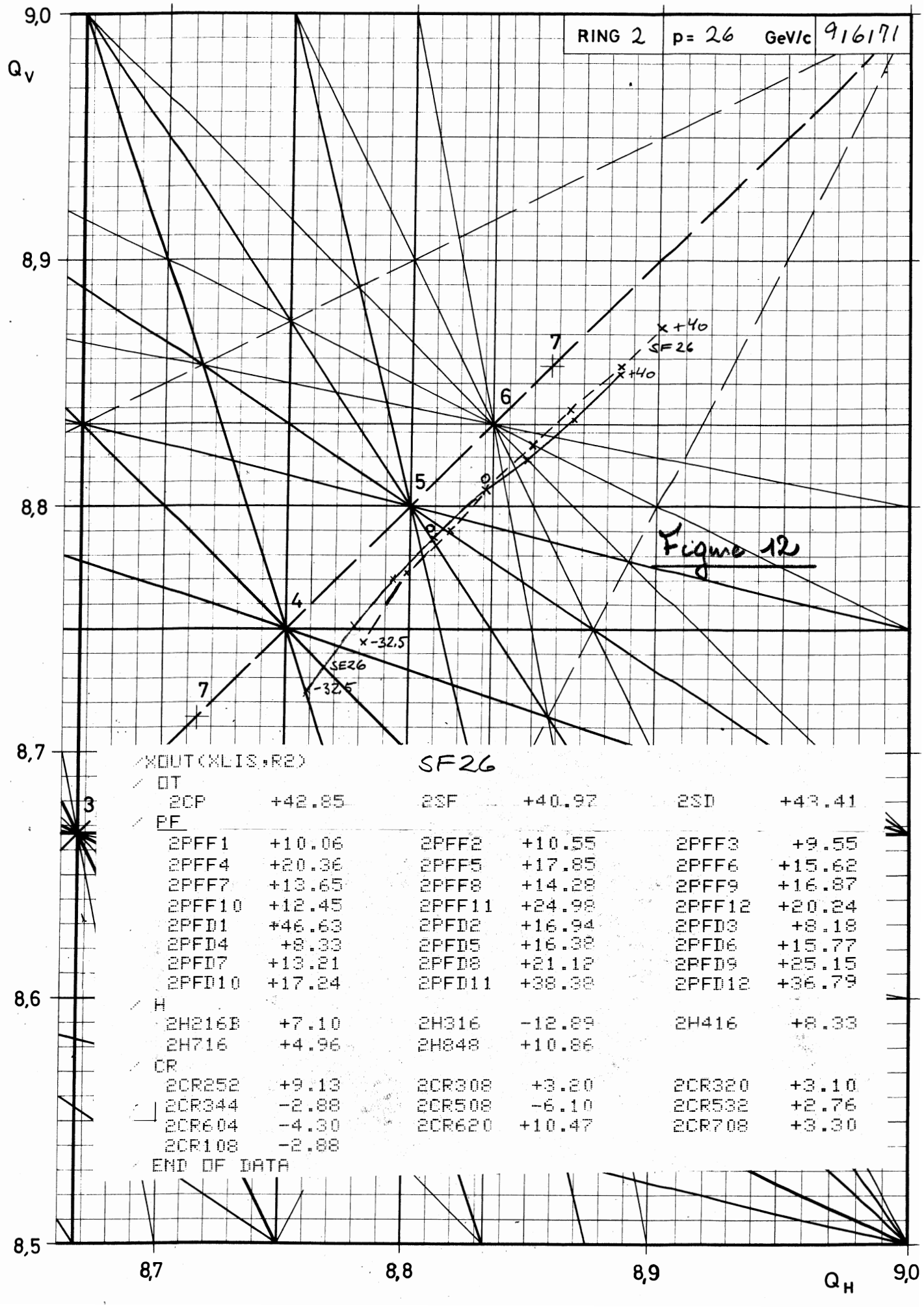

Figure 12

SF26

```
/XOUT(XLIS,R2)
/ QT
   2CF      +42.85      2SF      +40.97      2SD      +43.41
/ PF
   2PFF1    +10.06      2PFF2    +10.55      2PFF3     +9.55
   2PFF4    +20.36      2PFF5    +17.85      2PFF6    +15.62
   2PFF7    +13.65      2PFF8    +14.28      2PFF9    +16.87
   2PFF10   +12.45      2PFF11   +24.98      2PFF12   +20.24
   2PFD1    +46.63      2PFD2    +16.94      2PFD3     +8.18
   2PFD4     +8.33      2PFD5    +16.38      2PFD6    +15.77
   2PFD7    +13.21      2PFD8    +21.12      2PFD9    +25.15
   2PFD10   +17.24      2PFD11   +38.38      2PFD12   +36.79
/ H
   2H216B    +7.10      2H316    -12.89      2H416     +8.33
   2H716     +4.96      2H848    +10.86
/ CR
   2CR252    +9.13      2CR308    +3.20      2CR320    +3.10
   2CR344    -2.88      2CR508    -6.10      2CR532    +2.76
   2CR604    -4.30      2CR620   +10.47      2CR708    +3.30
   2CR108    -2.88
/ END OF DATA
```

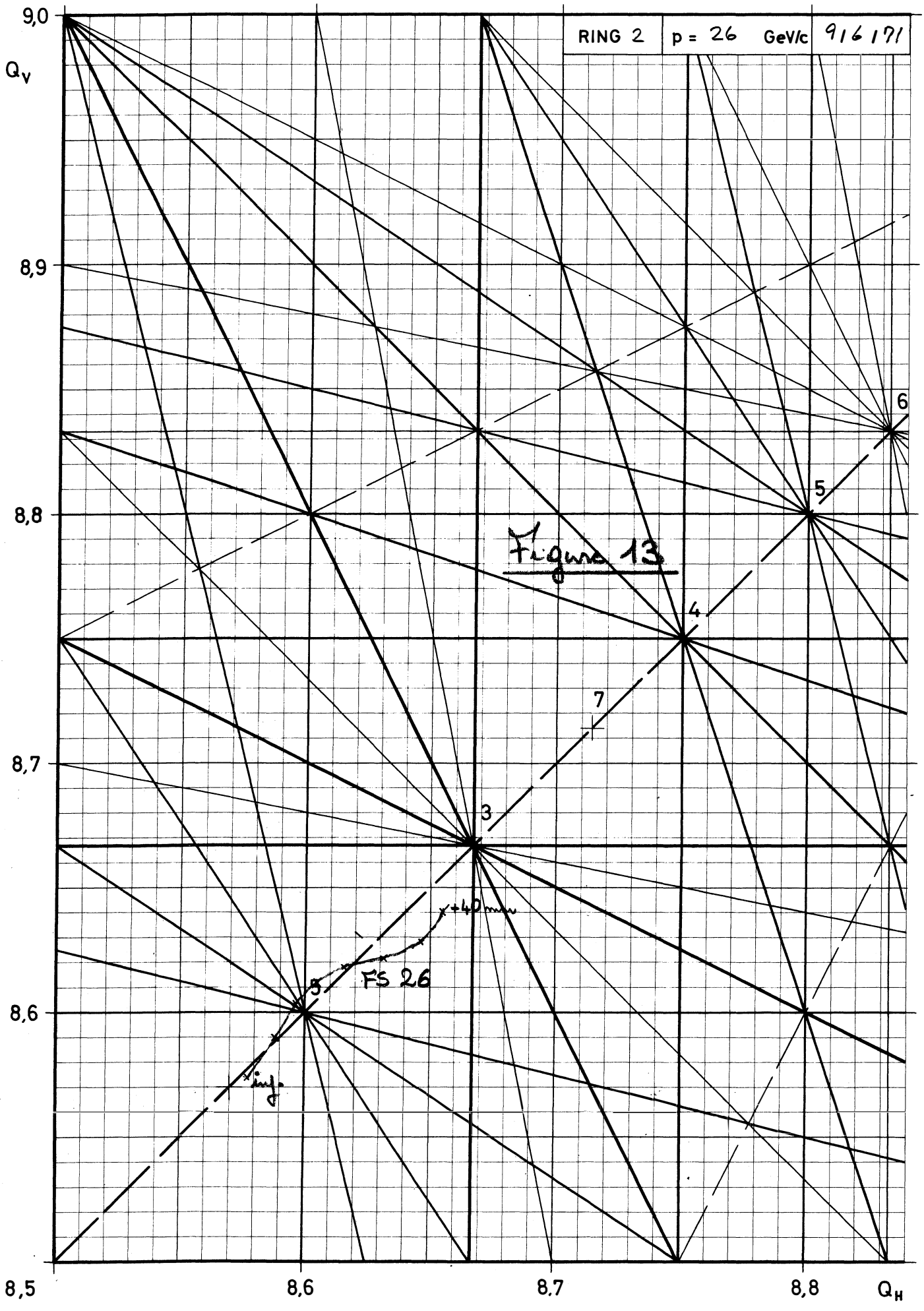
RING 2
p = 26 GeV/c
9 6 1 71
Q_V
9,0
8,9
8,8
8,7
8,6
8,5
8,6
8,7
8,8
Q_H
3
4
5
6
7
5
x+40mm
FS 26
x inj.

Figure 13